Cross section measurement of $e^+e^- \to K_S^0 K_L^0$ at $\sqrt{s} = 2.00 - 3.08$ GeV

M. Ablikim,[1] M. N. Achasov,[10,c] P. Adlarson,[64] S. Ahmed,[15] M. Albrecht,[4] A. Amoroso,[63a,63c] Q. An,[60,48] Anita,[21] X. H. Bai,[54] Y. Bai,[47] O. Bakina,[29] R. Baldini Ferroli,[23a] I. Balossino,[24a] Y. Ban,[38,k] K. Begzsuren,[26] J. V. Bennett,[5] N. Berger,[28] M. Bertani,[23a] D. Bettoni,[24a] F. Bianchi,[63a,63c] J. Biernat,[64] J. Bloms,[57] A. Bortone,[63a,63c] I. Boyko,[29] R. A. Briere,[5] H. Cai,[65] X. Cai,[1,48] A. Calcaterra,[23a] G. F. Cao,[1,52] N. Cao,[1,52] S. A. Cetin,[51b] J. F. Chang,[1,48] W. L. Chang,[1,52] G. Chelkov,[29,b] D. Y. Chen,[6] G. Chen,[1] H. S. Chen,[1,52] M. L. Chen,[1,48] S. J. Chen,[36] X. R. Chen,[25] Y. B. Chen,[1,48] Z. J. Chen,[20,l] W. S. Cheng,[63c] G. Cibinetto,[24a] F. Cossio,[63c] X. F. Cui,[37] H. L. Dai,[1,48] J. P. Dai,[42,g] X. C. Dai,[1,52] A. Dbeyssi,[15] R. B. de Boer,[4] D. Dedovich,[29] Z. Y. Deng,[1] A. Denig,[28] I. Denysenko,[29] M. Destefanis,[63a,63c] F. De Mori,[63a,63c] Y. Ding,[34] C. Dong,[37] J. Dong,[1,48] L. Y. Dong,[1,52] M. Y. Dong,[1,48,52] S. X. Du,[68] J. Fang,[1,48] S. S. Fang,[1,52] Y. Fang,[1] R. Farinelli,[24a] L. Fava,[63b,63c] F. Feldbauer,[4] G. Felici,[23a] C. Q. Feng,[60,48] M. Fritsch,[4] C. D. Fu,[1] Y. Fu,[1] X. L. Gao,[60,48] Y. Gao,[38,k] Y. Gao,[61] Y. G. Gao,[6] I. Garzia,[24a,24b] E. M. Gersabeck,[55] A. Gilman,[56] K. Goetzen,[11] L. Gong,[37] W. X. Gong,[1,48] W. Gradl,[28] M. Greco,[63a,63c] L. M. Gu,[36] M. H. Gu,[1,48] S. Gu,[2] Y. T. Gu,[13] C. Y. Guan,[1,52] A. Q. Guo,[22] L. B. Guo,[35] R. P. Guo,[40] Y. P. Guo,[9,h] Y. P. Guo,[28] A. Guskov,[29] S. Han,[65] T. T. Han,[41] T. Z. Han,[9,h] X. Q. Hao,[16] F. A. Harris,[53] K. L. He,[1,52] F. H. Heinsius,[4] T. Held,[4] Y. K. Heng,[1,48,52] M. Himmelreich,[11,f] T. Holtmann,[4] Y. R. Hou,[52] Z. L. Hou,[1] H. M. Hu,[1,52] J. F. Hu,[42,g] T. Hu,[1,48,52] Y. Hu,[1] G. S. Huang,[60,48] L. Q. Huang,[61] X. T. Huang,[41] Y. P. Huang,[1] Z. Huang,[38,k] N. Huesken,[57] T. Hussain,[62] W. Ikegami Andersson,[64] W. Imoehl,[22] M. Irshad,[60,48] S. Jaeger,[4] S. Janchiv,[26,j] Q. Ji,[1] Q. P. Ji,[16] X. B. Ji,[1,52] X. L. Ji,[1,48] H. B. Jiang,[41] X. S. Jiang,[1,48,52] X. Y. Jiang,[37] J. B. Jiao,[41] Z. Jiao,[18] S. Jin,[36] Y. Jin,[54] T. Johansson,[64] N. Kalantar-Nayestanaki,[31] X. S. Kang,[34] R. Kappert,[31] M. Kavatsyuk,[31] B. C. Ke,[43,1] I. K. Keshk,[4] A. Khoukaz,[57] P. Kiese,[28] R. Kiuchi,[1] R. Kliemt,[11] L. Koch,[30] O. B. Kolcu,[51b,e] B. Kopf,[4] M. Kuemmel,[4] M. Kuessner,[4] A. Kupsc,[64] M. G. Kurth,[1,52] W. Kühn,[30] J. J. Lane,[55] J. S. Lange,[30] P. Larin,[15] L. Lavezzi,[63c] H. Leithoff,[28] M. Lellmann,[28] T. Lenz,[28] C. Li,[39] C. H. Li,[33] Cheng Li,[60,48] D. M. Li,[68] F. Li,[1,48] G. Li,[1] H. B. Li,[1,52] H. J. Li,[9,h] J. L. Li,[41] J. Q. Li,[4] Ke Li,[1] L. K. Li,[1] Lei Li,[3] P. L. Li,[60,48] P. R. Li,[32] S. Y. Li,[50] W. D. Li,[1,52] W. G. Li,[1] X. H. Li,[60,48] X. L. Li,[41] Z. B. Li,[49] Z. Y. Li,[49] H. Liang,[1,52] H. Liang,[60,48] Y. F. Liang,[45] Y. T. Liang,[25] L. Z. Liao,[1,52] J. Libby,[21] C. X. Lin,[49] B. Liu,[42,g] B. J. Liu,[1] C. X. Liu,[1] D. Liu,[60,48] D. Y. Liu,[42,g] F. H. Liu,[44] Fang Liu,[1] Feng Liu,[6] H. B. Liu,[13] H. M. Liu,[1,52] Huanhuan Liu,[1] Huihui Liu,[17] J. B. Liu,[60,48] J. Y. Liu,[1,52] K. Liu,[1] K. Y. Liu,[34] Ke Liu,[6] L. Liu,[60,48] Q. Liu,[52] S. B. Liu,[60,48] Shuai Liu,[46] T. Liu,[1,52] X. Liu,[32] Y. B. Liu,[37] Z. A. Liu,[1,48,52] Z. Q. Liu,[41] Y. F. Long,[38,k] X. C. Lou,[1,48,52] F. X. Lu,[16] H. J. Lu,[18] J. D. Lu,[1,52] J. G. Lu,[1,48] X. L. Lu,[1] Y. Lu,[1] Y. P. Lu,[1,48] C. L. Luo,[35] M. X. Luo,[67] P. W. Luo,[49] T. Luo,[9,h] X. L. Luo,[1,48] S. Lusso,[63c] X. R. Lyu,[52] F. C. Ma,[34] H. L. Ma,[1] L. L. Ma,[41] M. M. Ma,[1,52] Q. M. Ma,[1] R. Q. Ma,[1,52] R. T. Ma,[52] X. N. Ma,[37] X. X. Ma,[1,52] X. Y. Ma,[1,48] Y. M. Ma,[41] F. E. Maas,[15] M. Maggiora,[63a,63c] S. Maldaner,[28] S. Malde,[58] Q. A. Malik,[62] A. Mangoni,[23b] Y. J. Mao,[38,k] Z. P. Mao,[1] S. Marcello,[63a,63c] Z. X. Meng,[54] J. G. Messchendorp,[31] G. Mezzadri,[24a] T. J. Min,[36] R. E. Mitchell,[22] X. H. Mo,[1,48,52] Y. J. Mo,[6] N. Yu. Muchnoi,[10,c] H. Muramatsu,[56] S. Nakhoul,[11,f] Y. Nefedov,[29] F. Nerling,[11,f] I. B. Nikolaev,[10,c] Z. Ning,[1,48] S. Nisar,[8,i] S. L. Olsen,[52] Q. Ouyang,[1,48,52] S. Pacetti,[23b,23c] X. Pan,[46] Y. Pan,[55] A. Pathak,[1] P. Patteri,[23a] M. Pelizaeus,[4] H. P. Peng,[60,48] K. Peters,[11,f] J. Pettersson,[64] J. L. Ping,[35] R. G. Ping,[1,52] A. Pitka,[4] R. Poling,[56] V. Prasad,[60,48] H. Qi,[60,48] H. R. Qi,[50] M. Qi,[36] T. Y. Qi,[2] S. Qian,[1,48] W.-B. Qian,[52] Z. Qian,[49] C. F. Qiao,[52] L. Q. Qin,[12] X. S. Qin,[4] Z. H. Qin,[1,48] J. F. Qiu,[1] S. Q. Qu,[37] K. H. Rashid,[62] K. Ravindran,[21] C. F. Redmer,[28] A. Rivetti,[63c] V. Rodin,[31] M. Rolo,[63c] G. Rong,[1,52] Ch. Rosner,[15] M. Rump,[57] A. Sarantsev,[29,d] Y. Schelhaas,[28] C. Schnier,[4] K. Schoenning,[64] D. C. Shan,[46] W. Shan,[19] X. Y. Shan,[60,48] M. Shao,[60,48] C. P. Shen,[2,9] P. X. Shen,[37] X. Y. Shen,[1,52] H. C. Shi,[60,48] R. S. Shi,[1,52] X. Shi,[1,48] X. D. Shi,[60,48] J. J. Song,[41] Q. Q. Song,[60,48] W. M. Song,[27] Y. X. Song,[38,k] S. Sosio,[63a,63c] S. Spataro,[63a,63c] F. F. Sui,[41] G. X. Sun,[1] J. F. Sun,[16] L. Sun,[65] S. S. Sun,[1,52] T. Sun,[1,52] W. Y. Sun,[35] X. Sun,[20,l] Y. J. Sun,[60,48] Y. K. Sun,[60,48] Y. Z. Sun,[1] Z. T. Sun,[1] Y. H. Tan,[65] Y. X. Tan,[60,48] C. J. Tang,[45] G. Y. Tang,[1] J. Tang,[49] V. Thoren,[64] B. Tsednee,[26] I. Uman,[51d] B. Wang,[1] B. L. Wang,[52] C. W. Wang,[36] D. Y. Wang,[38,k] H. P. Wang,[1,52] K. Wang,[1,48] L. L. Wang,[1] M. Wang,[41] M. Z. Wang,[38,k] Meng Wang,[1,52] W. H. Wang,[65] W. P. Wang,[60,48] X. Wang,[38,k] X. F. Wang,[32] X. L. Wang,[9,h] Y. Wang,[60,48] Y. Wang,[49] Y. D. Wang,[15] Y. F. Wang,[1,48,52] Y. Q. Wang,[1] Z. Wang,[1,48] Z. Y. Wang,[1] Ziyi Wang,[52] Zongyuan Wang,[1,52] D. H. Wei,[12] P. Weidenkaff,[28] F. Weidner,[57] S. P. Wen,[1] D. J. White,[55] U. Wiedner,[4] G. Wilkinson,[58] M. Wolke,[64] L. Wollenberg,[4] J. F. Wu,[1,52] L. H. Wu,[1] L. J. Wu,[1,52] X. Wu,[9,h] Z. Wu,[1,48] L. Xia,[60,48] H. Xiao,[9,h] S. Y. Xiao,[1] Y. J. Xiao,[1,52] Z. J. Xiao,[35] X. H. Xie,[38,k] Y. G. Xie,[1,48] Y. H. Xie,[6] T. Y. Xing,[1,52] X. A. Xiong,[1,52] G. F. Xu,[1] J. J. Xu,[36] Q. J. Xu,[14] W. Xu,[1,52] X. P. Xu,[46] L. Yan,[63a,63c] L. Yan,[9,h] W. B. Yan,[60,48] W. C. Yan,[68] Xu Yan,[46] H. J. Yang,[42,g] H. X. Yang,[1] L. Yang,[65] R. X. Yang,[60,48] S. L. Yang,[1,52] Y. H. Yang,[36] Y. X. Yang,[12] Yifan Yang,[1,52] Zhi Yang,[25] M. Ye,[1,48] M. H. Ye,[7] J. H. Yin,[1] Z. Y. You,[49] B. X. Yu,[1,48,52] C. X. Yu,[37] G. Yu,[1,52] J. S. Yu,[20,l] T. Yu,[61] C. Z. Yuan,[1,52] W. Yuan,[63a,63c] X. Q. Yuan,[38,k] Y. Yuan,[1] Z. Y. Yuan,[49] C. X. Yue,[33] A. Yuncu,[51b,a] A. A. Zafar,[62] Y. Zeng,[20,l] B. X. Zhang,[1] Guangyi Zhang,[16] H. H. Zhang,[49] H. Y. Zhang,[1,48] J. L. Zhang,[66] J. Q. Zhang,[4] J. W. Zhang,[1,48,52] J. Y. Zhang,[1] J. Z. Zhang,[1,52] Jianyu Zhang,[1,52] Jiawei Zhang,[1,52] L. Zhang,[1] Lei Zhang,[36] S. Zhang,[49] S. F. Zhang,[36]

T. J. Zhang,[42,g] X. Y. Zhang,[41] Y. Zhang,[58] Y. H. Zhang,[1,48] Y. T. Zhang,[60,48] Yan Zhang,[60,48] Yao Zhang,[1] Yi Zhang,[9,h] Z. H. Zhang,[6] Z. Y. Zhang,[65] G. Zhao,[1] J. Zhao,[33] J. Y. Zhao,[1,52] J. Z. Zhao,[1,48] Lei Zhao,[60,48] Ling Zhao,[1] M. G. Zhao,[37] Q. Zhao,[1] S. J. Zhao,[68] Y. B. Zhao,[1,48] Y. X. Zhao,[25] Z. G. Zhao,[60,48] A. Zhemchugov,[29,b] B. Zheng,[61] J. P. Zheng,[1,48] Y. Zheng,[38,k] Y. H. Zheng,[52] B. Zhong,[35] C. Zhong,[61] L. P. Zhou,[1,52] Q. Zhou,[1,52] X. Zhou,[65] X. K. Zhou,[52] X. R. Zhou,[60,48] A. N. Zhu,[1,52] J. Zhu,[37] K. Zhu,[1] K. J. Zhu,[1,48,52] S. H. Zhu,[59] W. J. Zhu,[37] X. L. Zhu,[50] Y. C. Zhu,[60,48] Z. A. Zhu,[1,52] B. S. Zou,[1] and J. H. Zou[1]

(BESIII Collaboration)

[1]*Institute of High Energy Physics, Beijing 100049, People's Republic of China*
[2]*Beihang University, Beijing 100191, People's Republic of China*
[3]*Beijing Institute of Petrochemical Technology, Beijing 102617, People's Republic of China*
[4]*Bochum Ruhr-University, D-44780 Bochum, Germany*
[5]*Carnegie Mellon University, Pittsburgh, Pennsylvania 15213, USA*
[6]*Central China Normal University, Wuhan 430079, People's Republic of China*
[7]*China Center of Advanced Science and Technology, Beijing 100190, People's Republic of China*
[8]*COMSATS University Islamabad, Lahore Campus, Defence Road, Off Raiwind Road, 54000 Lahore, Pakistan*
[9]*Fudan University, Shanghai 200443, People's Republic of China*
[10]*G.I. Budker Institute of Nuclear Physics SB RAS (BINP), Novosibirsk 630090, Russia*
[11]*GSI Helmholtzcentre for Heavy Ion Research GmbH, D-64291 Darmstadt, Germany*
[12]*Guangxi Normal University, Guilin 541004, People's Republic of China*
[13]*Guangxi University, Nanning 530004, People's Republic of China*
[14]*Hangzhou Normal University, Hangzhou 310036, People's Republic of China*
[15]*Helmholtz Institute Mainz, Johann-Joachim-Becher-Weg 45, D-55099 Mainz, Germany*
[16]*Henan Normal University, Xinxiang 453007, People's Republic of China*
[17]*Henan University of Science and Technology, Luoyang 471003, People's Republic of China*
[18]*Huangshan College, Huangshan 245000, People's Republic of China*
[19]*Hunan Normal University, Changsha 410081, People's Republic of China*
[20]*Hunan University, Changsha 410082, People's Republic of China*
[21]*Indian Institute of Technology Madras, Chennai 600036, India*
[22]*Indiana University, Bloomington, Indiana 47405, USA*
[23a]*INFN Laboratori Nazionali di Frascati, I-00044 Frascati, Italy*
[23b]*INFN Sezione di Perugia, I-06100 Perugia, Italy*
[23c]*University of Perugia, I-06100 Perugia, Italy*
[24a]*INFN Sezione di Ferrara, I-44122 Ferrara, Italy*
[24b]*University of Ferrara, I-44122 Ferrara, Italy*
[25]*Institute of Modern Physics, Lanzhou 730000, People's Republic of China*
[26]*Institute of Physics and Technology, Peace Avenue 54B, Ulaanbaatar 13330, Mongolia*
[27]*Jilin University, Changchun 130012, People's Republic of China*
[28]*Johannes Gutenberg University of Mainz, Johann-Joachim-Becher-Weg 45, D-55099 Mainz, Germany*
[29]*Joint Institute for Nuclear Research, 141980 Dubna, Moscow region, Russia*
[30]*Justus-Liebig-Universitaet Giessen, II. Physikalisches Institut, Heinrich-Buff-Ring 16, D-35392 Giessen, Germany*
[31]*KVI-CART, University of Groningen, NL-9747 AA Groningen, The Netherlands*
[32]*Lanzhou University, Lanzhou 730000, People's Republic of China*
[33]*Liaoning Normal University, Dalian 116029, People's Republic of China*
[34]*Liaoning University, Shenyang 110036, People's Republic of China*
[35]*Nanjing Normal University, Nanjing 210023, People's Republic of China*
[36]*Nanjing University, Nanjing 210093, People's Republic of China*
[37]*Nankai University, Tianjin 300071, People's Republic of China*
[38]*Peking University, Beijing 100871, People's Republic of China*
[39]*Qufu Normal University, Qufu 273165, People's Republic of China*
[40]*Shandong Normal University, Jinan 250014, People's Republic of China*
[41]*Shandong University, Jinan 250100, People's Republic of China*
[42]*Shanghai Jiao Tong University, Shanghai 200240, People's Republic of China*
[43]*Shanxi Normal University, Linfen 041004, People's Republic of China*
[44]*Shanxi University, Taiyuan 030006, People's Republic of China*
[45]*Sichuan University, Chengdu 610064, People's Republic of China*

[46]*Soochow University, Suzhou 215006, People's Republic of China*
[47]*Southeast University, Nanjing 211100, People's Republic of China*
[48]*State Key Laboratory of Particle Detection and Electronics, Beijing 100049, Hefei 230026, People's Republic of China*
[49]*Sun Yat-Sen University, Guangzhou 510275, People's Republic of China*
[50]*Tsinghua University, Beijing 100084, People's Republic of China*
[51a]*Ankara University, 06100 Tandogan, Ankara, Turkey*
[51b]*Istanbul Bilgi University, 34060 Eyup, Istanbul, Turkey*
[51c]*Uludag University, 16059 Bursa, Turkey*
[51d]*Near East University, 99138 Nicosia, North Cyprus, Mersin 10, Turkey*
[52]*University of Chinese Academy of Sciences, Beijing 100049, People's Republic of China*
[53]*University of Hawaii, Honolulu, Hawaii 96822, USA*
[54]*University of Jinan, Jinan 250022, People's Republic of China*
[55]*University of Manchester, Oxford Road, Manchester M13 9PL, United Kingdom*
[56]*University of Minnesota, Minneapolis, Minnesota 55455, USA*
[57]*University of Muenster, Wilhelm-Klemm-Straße 9, 48149 Muenster, Germany*
[58]*University of Oxford, Keble Rd, Oxford OX13RH, United Kingdom*
[59]*University of Science and Technology Liaoning, Anshan 114051, People's Republic of China*
[60]*University of Science and Technology of China, Hefei 230026, People's Republic of China*
[61]*University of South China, Hengyang 421001, People's Republic of China*
[62]*University of the Punjab, Lahore-54590, Pakistan*
[63a]*University of Turin, I-10125 Turin, Italy;*
[63b]*University of Eastern Piedmont, I-15121 Alessandria, Italy*
[63c]*INFN, I-10125 Turin, Italy*
[64]*Uppsala University, Box 516, SE-75120 Uppsala, Sweden*
[65]*Wuhan University, Wuhan 430072, People's Republic of China*
[66]*Xinyang Normal University, Xinyang 464000, People's Republic of China*
[67]*Zhejiang University, Hangzhou 310027, People's Republic of China*
[68]*Zhengzhou University, Zhengzhou 450001, People's Republic of China*

(Received 31 May 2021; accepted 15 October 2021; published 29 November 2021)

The cross sections of the process $e^+e^- \to K_S^0 K_L^0$ are measured at fifteen center-of-mass energies $\sqrt{s}$ from 2.00 to 3.08 GeV with a total integrated luminosity of 582 pb^{-1} and using the BESIII detector at the Beijing Electron Positron Collider. The results are found to be consistent with those obtained by *BABAR*. A resonant structure around 2.2 GeV is observed, with a mass and width of $2273.7 \pm 5.7 \pm 19.3\ \mathrm{MeV}/c^2$ and $86 \pm 44 \pm 51$ MeV, respectively, where the first uncertainties are statistical and the second ones are systematic. The product of its radiative width ($\Gamma_{e^+e^-}$) with its branching fraction to $K_S^0 K_L^0$ ($Br_{K_S^0 K_L^0}$) is $0.9 \pm 0.6 \pm 0.7$ eV.

DOI: 10.1103/PhysRevD.104.092014

[a]Also at Bogazici University, 34342 Istanbul, Turkey.
[b]Also at the Moscow Institute of Physics and Technology, Moscow 141700, Russia.
[c]Also at the Novosibirsk State University, Novosibirsk 630090, Russia.
[d]Also at the NRC "Kurchatov Institute", PNPI, 188300 Gatchina, Russia.
[e]Also at Istanbul Arel University, 34295 Istanbul, Turkey.
[f]Also at Goethe University Frankfurt, 60323 Frankfurt am Main, Germany.
[g]Also at Key Laboratory for Particle Physics, Astrophysics and Cosmology, Ministry of Education; Shanghai Key Laboratory for Particle Physics and Cosmology; Institute of Nuclear and Particle Physics, Shanghai 200240, People's Republic of China.
[h]Also at Key Laboratory of Nuclear Physics and Ion-beam Application (MOE) and Institute of Modern Physics, Fudan University, Shanghai 200443, People's Republic of China.
[i]Also at Harvard University, Department of Physics, Cambridge, Massachusetts 02138, USA.
[j]Present address: Institute of Physics and Technology, Peace Avenue 54B, Ulaanbaatar 13330, Mongolia.
[k]Also at State Key Laboratory of Nuclear Physics and Technology, Peking University, Beijing 100871, People's Republic of China.
[l]School of Physics and Electronics, Hunan University, Changsha 410082, China.

I. INTRODUCTION

Among the light unflavored mesons, the strangeonium-like state $\phi(2170)$ is particularly interesting. It was first reported in $e^+e^- \to \gamma_{ISR}\phi f_0(980)$ by the *BABAR* Collaboration [1], and then confirmed in $J/\psi \to \eta\phi f_0(980)$ by the BESII Collaboration [2] and in the $e^+e^- \to \phi f_0(980)$ and $\phi\pi^+\pi^-$ processes by the Belle Collaboration [3]. Subsequently, the $\phi(2170)$ has been studied extensively by *BABAR* [1,4–6], Belle [3], BESII [2], and BESIII [7–15].

Initially, the strangeonium-like state $\phi(2170)$ was only observed in hidden-strange decays, which makes its nature mysterious. Different interpretations have been proposed. In Refs. [16–22], the $\phi(2170)$ is considered to be a tetraquark, while in Refs. [23,24], it is considered as an $s\bar{s}g$ hybrid state. Lattice QCD [25] and QCD sum rule [26] investigations disfavor the $s\bar{s}g$ hybrid interpretation. Considering the near threshold location of the $\phi(2170)$, various hadronic molecular possibilities have been proposed, such as $\Lambda\bar{\Lambda}$ baryonium [27–29], a $\phi K\bar{K}$ [30] or a $\phi f_0(980)$ [31] resonance. Besides these exotic interpretations, the $\phi(2170)$ has been considered to be conventional strangeonium, corresponding to 3^3S_1 [32,33] or 2^3D_1 [23,24,33–36] states. The predicted decay rates of $\phi(2170) \to K\bar{K}$ differ among these theoretical interpretations. For example, the branching fraction is predicted to be 5%–10% under the assumption of a 2^3D_1 state [24,35] but close to zero in the case of an $s\bar{s}g$ or $3^3Ss\bar{s}$ [23] state. Therefore, an experimental measurement of the branching fraction of $\phi(2170) \to K\bar{K}$ provides crucial information to distinguish between the different interpretations.

Recently, the cross sections for $e^+e^- \to K^+K^-$ were measured by the BESIII and *BABAR* Collaborations [13,37]. A structure near 2.2 GeV was reported with a mass (width) differing from the world averaged parameters of the $\phi(2170)$ by 3σ (2σ). In addition, cross sections of the process $e^+e^- \to K_S^0K_L^0$ were measured by the *BABAR* Collaboration for center-of-mass (c.m.) energies in the range between 1.98 and 2.54 GeV [37]. In this case, however, no significant structure around 2.2 GeV was observed. We note that the observed peak at 2.2 GeV in the $e^+e^- \to K^+K^-$ channel is found to be compatible with the $\phi(2170)$ resonance parameters once one accounts in the fit of the BESIII cross section data for a possible interference between the direct coupling and the vector resonance intermediate contribution [38]. The interpretation is, however, ambiguous since the structure can similarly be explained as an ω-like state [39]. In general, considering the interferences between resonance and nonresonance contributions, additional information from other processes, such as $e^+e^- \to K_S^0K_L^0$, is needed. Although, this process has been investigated in the past by the DM1 [40], OLYa [41], CDM2 [42–44], SND [45,46] and *BABAR* [37,47] Collaborations, these measurements mainly focused on the energy region below 2.0 GeV.

In this work, we present Born cross section measurements of the process $e^+e^- \to K_S^0K_L^0$. The results obtained in the overlapping c.m. region from 2.00–2.54 GeV are compared to previous measurements by *BABAR* [37]. Moreover, we present, for the first time, Born cross section measurements taken in the interval from 2.54 to 3.08 GeV. A fit is applied to the cross section measurements of the $e^+e^- \to K_S^0K_L^0$ process, and the resonant structure result is compared with that found by BESIII [13] and *BABAR* [37] in $e^+e^- \to K^+K^-$.

II. DETECTOR, DATA SAMPLE AND MONTE CARLO SIMULATION

The BESIII detector is a magnetic spectrometer [48] located at BEPCII [49]. The cylindrical core of the BESIII detector consists of a helium-based multilayer drift chamber (MDC), a plastic scintillator time-of-flight system (TOF), and a CsI(Tl) electromagnetic calorimeter (EMC), which are all enclosed in a superconducting solenoidal magnet providing a 1.0 T magnetic field. The solenoid is supported by an octagonal flux-return yoke with resistive plate counter muon identifier modules interleaved with steel. The acceptance of charged particles and photons is 93% over 4π solid angle. The charged-particle momentum resolution at 1 GeV/c is 0.5%, and the dE/dx resolution is 6% for the electrons from Bhabha scattering. The EMC measures photon energies with a resolution of 2.5% (5%) at 1 GeV in the barrel (end cap) region. The time resolution of the TOF barrel part is 68 ps, while that of the end cap part is 110 ps.

The data samples used in this work are collected by the BESIII detector at fifteen c.m. energies between 2.00 and 3.08 GeV with an integrated luminosity of 582 pb^{-1} [50,51].

Monte Carlo (MC) samples simulated with a model of the complete detector are used to determine detection efficiency, optimize event selection criteria, and estimate backgrounds. Detector geometry, material description, propagation and interactions with the detector of the final-state particles are handled by GEANT4-based [52] simulation software, BESIII Object Oriented Simulation Tool [53].

Signal and background samples are generated at each c.m. energy ($\sqrt{s}$). Signal MC simulations of $e^+e^- \to K_S^0K_L^0$ and $K_S^0 \to \pi^+\pi^-$ are generated with ConExc [54]. Nonhadronic backgrounds including continuum processes of $e^+e^- \to e^+e^-$, $e^+e^- \to \gamma\gamma$ and $e^+e^- \to \mu^+\mu^-$ are generated with Babayaga [55]. Inclusive hadronic samples ($e^+e^- \to q\bar{q}$) are generated with Luarlw [56]. Two-photon samples are generated with BesTwoGam [57].

III. EVENT SELECTION AND BACKGROUND ANALYSIS

The momentum of the K_S^0 meson is reconstructed from its $K_S^0 \to \pi^+\pi^-$ decay. Events containing the reconstructed

K_S^0 candidates are retained for further analysis. The K_L^0 meson is not detected directly; because of the two-body decay, its presence is inferred by a requirement on the K_S^0 candidate momentum. To select signal candidates, the following criteria are applied:

(i) Exactly two oppositely charged tracks are required without any requirement on neutral particles. The distance of closest approach of the track with respect to the interaction point is required to be less than 20 cm along the beam direction (z axis of the BESIII coordinate system), while no requirement is made with respect to the transverse direction. Tracks are required to be within the acceptance of the MDC, i.e., $|\cos\theta| < 0.93$, where θ is the polar angle between the track and the z axis. A vertex fit is applied to constrain the two tracks to a common vertex, and subsequently a secondary vertex fit is performed to determine the flight distance L and corresponding uncertainty δL, where L corresponds to the separation between the secondary vertex and the interaction point. The typical value of δL is $\sim$1 mm in the vertex reconstruction of the K_S^0 candidates [58,59]. We require $L/\delta L$ to be larger than 2, as illustrated by the green vertical line in Fig. 1. The invariant mass of the two tracks ($m_{\pi^+\pi^-}$), where the tracks are treated as π^+ and π^- candidates, is required to satisfy $|m_{\pi^+\pi^-} - m_{K_S^0}| < 35\ \mathrm{MeV}/c^2$, where $m_{K_S^0} = 497.611\ \mathrm{MeV}/c^2$ is the mass of K_S^0 taken from the Particle Data Group (PDG) [60]. The signal yields are determined from fits to the invariant-mass distributions, as discussed in Sec. IV.

(ii) To reject backgrounds from the $e^+e^- \to e^+e^-$ and $e^+e^- \to \gamma\gamma$ processes, we require the ratio E/cp between the deposited energy in the EMC (E) and the momentum measured by the MDC (p) to be less than 0.8.

(iii) $|p_{\pi^+\pi^-} - p_{K_S^0}| < \sigma_p$ must be satisfied to suppress backgrounds from three (or more) body decays, where $p_{\pi^+\pi^-}$ is the sum of the reconstructed momenta of the π^+ and π^- candidates, $p_{K_S^0} = \sqrt{\frac{s}{4} - (m_{K_S^0})^2}$ is the expected K_S^0 momentum, and $\sigma_p = 15\ \mathrm{MeV}/c$ is the momentum resolution of the reconstructed K_S^0 determined using data obtained from the signal MC simulation. The $p_{\pi^+\pi^-}$ distribution is shown in Fig. 2.

For the nonhadronic background and the two-photon process, MC studies indicate that they contribute less than 5% in the region $|m_{\pi^+\pi^-} - m_{K_S^0}| < 3\sigma_{K_S^0}$ at low c.m. energies (< 2.396 GeV) and by at most 20% at 3.080 GeV, without peaking structure. $\sigma_{K_S^0} = 4\ \mathrm{MeV}/c^2$ is the mass resolution of the pion pair determined by fitting the predicted distribution from the signal MC simulation. For the hadronic background, a detailed event type analysis with a generic tool, TopoAna [61], shows that the following four channels are dominant: $e^+e^- \to K_S^0 K_L^0 \pi^0$, $e^+e^- \to \pi^+\pi^-\pi^+\pi^-$, $e^+e^- \to \pi^+\pi^-\pi^0$ and $e^+e^- \to (\gamma)\pi^+\pi^-$. A further study using

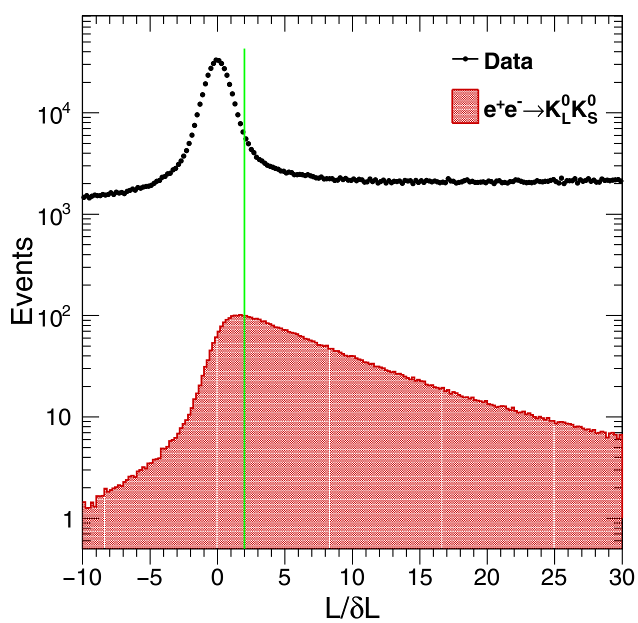

FIG. 1. $L/\delta L$ distribution for data taken at $\sqrt{s} = 2.125$ GeV. Dots refer to data and the shaded area corresponds to simulated signal events normalized to the integrated luminosity of the data. The (green) vertical line indicates the requirement that is applied to select signal candidate events.

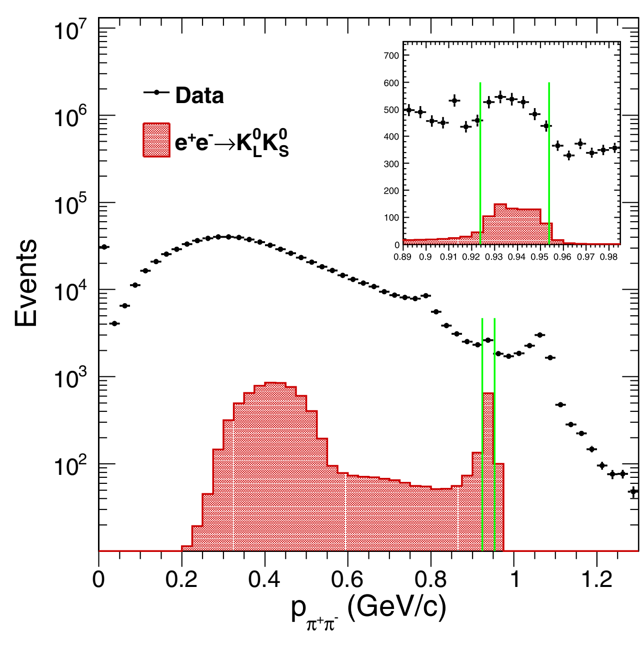

FIG. 2. $p_{\pi^+\pi^-}$ momentum distribution taken at $\sqrt{s} = 2.125$ GeV. Dots refer to data and the shaded area depicts simulated signal events normalized to the integrated luminosity of the data. The wide peak on the left side in the simulated signal distribution stems from events that undergo initial-state radiation. The vertical lines indicate the window of the signal region. Inset zooms in the signal region.

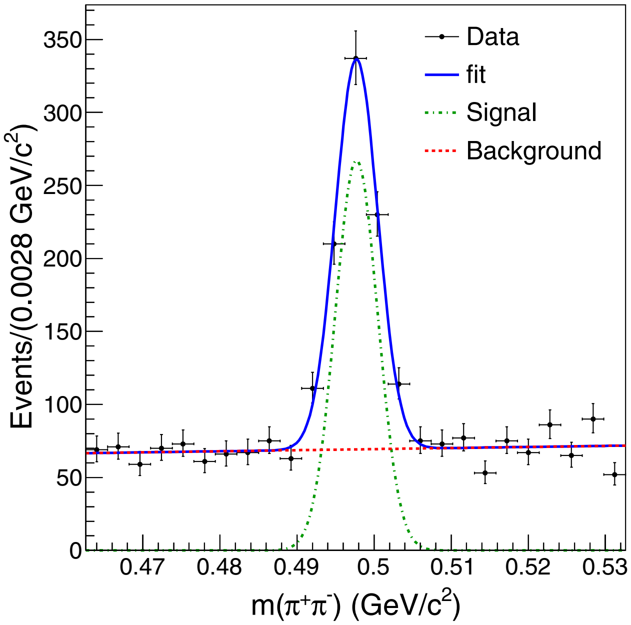

FIG. 3. $m_{\pi^+\pi^-}$ distribution of data taken at $\sqrt{s} = 2.125$ GeV. The solid curve denotes the best fit through the data of the complete model, whereby the dash-dotted and dashed lines are the corresponding signal and background components, respectively.

exclusive hadronic MC simulations shows that only at $\sqrt{s} = 3.080$ GeV can a peaking background be expected from the process $e^+e^- \to K_S^0 K_L^0 \pi^0$. The effect to the systematic uncertainty will be further discussed in Sec. V.

IV. CROSS SECTION

Born cross sections (σ_B) are obtained at each energy point by

$$\sigma_B = \frac{N_{sig}}{\epsilon(1+\delta)\mathcal{L}}, \tag{1}$$

where N_{sig} is the signal yield, ϵ is the detection efficiency, $1+\delta$ is the correction factor including vacuum polarization (VP) and initial-state radiation (ISR) effects, and $\mathcal{L}$ is the integrated luminosity measured using large-angle Bhabha scattering events with the method elucidated in Ref. [50]. The branching ratio of the decay $K_S^0 \to \pi^+\pi^-$ has been incorporated into ϵ.

The signal yields are determined with an unbinned maximum-likelihood fit to the invariant-mass distribution of $\pi^+\pi^-$ pairs of the selected events obtained for each c.m. energy point, where the signal shape is described by a Gaussian function and the background is represented with a zero-order Chebychev polynomial. The fit range is taken with a window of more than $8\sigma_{K_S^0}$ around the signal K_S^0. The mass and width of the Gaussian function are fixed to $m_{K_S^0}$ and $\sigma_{K_S^0}$, respectively, for most of the c.m. energy points. Only for the two datasets taken with the highest statistics at $\sqrt{s} = 2.000$ GeV and $\sqrt{s} = 2.125$ GeV) are the mass and width taken as free parameters. The signal and background yields are set free for all c.m. energies. As an example, Fig. 3 illustrates the $m_{\pi^+\pi^-}$ distribution together with the corresponding fit result for data taken at $\sqrt{s} = 2.125$ GeV.

Both ϵ and $1+\delta$ depend on the line shape of the cross sections and are determined via an iterative procedure. In the first iteration, the cross sections from 2.00 to 3.08 GeV are obtained and taken as initial inputs. The cross sections below 2.00 GeV are provided by previous experiments [40–47] and fitted together with our measurements above 2.00 GeV. The parameters ϵ and $1+\delta$ are calculated according to the fit curve at each c.m. energy and are

TABLE I. Born cross sections of the $e^+e^- \to K_S^0 K_L^0$ process. The columns N_{sig} and N_{bkg} show the numbers of signal and background events determined by fitting the $m_{\pi^+\pi^-}$ distribution. The detection efficiency ϵ, ISR and VP correction factor $1+\delta$, and the integrated luminosity $\mathcal{L}$ are summarized in the 4th, 5th, and 6th column, respectively. The values presented in the column labeled with σ_B correspond to the measured Born cross section, where the first uncertainty is statistical and the second one is systematic.

$\sqrt{s}$ (GeV)	N_{sig}	N_{bkg}	$\epsilon(\times 10^{-4})$	$(1+\delta)$	$\mathcal{L}(\mathrm{pb}^{-1})$	$\sigma_B(\times 10^{-3})$(nb)
2.0000	185 ± 18	341 ± 22	541.2	6.09	10.1	$53.9 \pm 5.2 \pm 4.1$
2.0500	51 ± 9	115 ± 12	448.8	7.48	3.34	$44.0 \pm 7.8 \pm 3.7$
2.1000	101 ± 13	252 ± 18	289.6	11.77	12.2	$23.5 \pm 3.0 \pm 3.6$
2.1250	658 ± 34	1731 ± 47	230.2	14.77	108.	$17.2 \pm 0.9 \pm 1.4$
2.1500	14 ± 6	101 ± 11	198.1	16.85	2.84	$14.2 \pm 6.1 \pm 1.3$
2.1750	67 ± 10	125 ± 13	213.0	15.59	10.6	$18.3 \pm 2.7 \pm 2.6$
2.2000	81 ± 11	146 ± 14	266.9	12.13	13.7	$17.6 \pm 2.4 \pm 1.2$
2.2324	98 ± 12	133 ± 13	360.9	9.03	11.9	$24.4 \pm 3.0 \pm 2.1$
2.3094	116 ± 13	171 ± 15	259.4	13.04	21.1	$15.6 \pm 1.8 \pm 1.0$
2.3864	27 ± 7	78 ± 10	82.0	40.84	22.5	$3.4 \pm 0.9 \pm 0.7$
2.3960	91 ± 13	309 ± 20	77.4	43.12	66.9	$3.9 \pm 0.6 \pm 0.5$
2.6444	52 ± 9	90 ± 11	51.8	59.69	33.7	$4.8 \pm 0.8 \pm 0.7$
2.6464	57 ± 9	70 ± 10	51.8	59.30	34.0	$5.2 \pm 0.8 \pm 0.3$
2.9000	43 ± 9	91 ± 11	42.9	68.07	105.	$1.4 \pm 0.3 \pm 0.2$
3.0800	42 ± 8	85 ± 11	34.7	77.79	126.	$1.3 \pm 0.2 \pm 0.2$

taken as input for the next iteration. The procedure is repeated until the measured Born cross sections converge.

Results are summarized in Table I with both statistical and systematic uncertainties given in the last column. The systematic uncertainties are discussed in Sec. V.

V. SYSTEMATIC UNCERTAINTIES AND LINE SHAPE

A. Systematic uncertainties of the Born cross sections

Several sources of the systematic uncertainties are estimated at each c.m. energy point, including uncertainties in the determination of the K_S^0 selection efficiency, in applying the E/cp requirement, in the ISR and VP correction factors, in the integrated luminosity, and in the fit procedure that was used to determine the signal yield. The uncertainty in the $K_S^0 \to \pi^+\pi^-$ branching ratio is only 0.07% [60], which is considered to be negligible in this study.

The systematic uncertainty of the K_S^0 selection efficiency is obtained using the control samples $J/\psi \to K^*(892)^{\mp}K^{\pm}$, $K^*(892)^{\mp} \to K_S^0\pi^{\mp}$ and $J/\psi \to \phi K_S^0 K^{\mp}\pi^{\pm}$, and the uncertainties are between 2.2% and 4.8% depending on the reconstructed K_S^0 momentum [62]. The uncertainty from the E/cp requirement is estimated as 0.75% for each c.m. energy by utilizing the control sample $J/\psi \to \pi^+\pi^-\pi^0$. The uncertainties of the signal shape description, background model and fit range determine the uncertainties of the signal yields. The uncertainty from the signal shape description is estimated by replacing the Gaussian function to the shape predicted by the distribution of the MC simulation. The uncertainty due to the background model is determined by replacing the background function with a first-order Chebychev polynomial. The uncertainty associated to the fit range is estimated by enlarging or reducing the fit range with an amount corresponding to the $\sigma_{K_S^0}$. For these systematic uncertainty studies, we applied the same strategy for the parameter settings as described in Sec. IV. Namely, signal and background yields are set free for all c.m. energies. The mass and width of the Gaussian function are fixed to $m_{K_S^0}$ and $\sigma_{K_S^0}$, respectively, for most of the c.m. energy points except for the two energies with the highest statistics (2.000 and 2.125 GeV). In those cases, the mass and width of the signal are both taken as free parameters.

The systematic uncertainty of $\epsilon \times (1+\delta)$ is obtained by fluctuating randomly all the fit parameters within the iteration procedure by one σ and taking into account the correlations among the parameters. The distribution of the randomly produced $\epsilon \times (1+\delta)$ is fitted by a Gaussian function, and the width of the fitted parameter is defined as the systematic uncertainty of $\epsilon \times (1+\delta)$. The luminosity is measured using large-angle Bhabha scattering events, with an uncertainty of 0.9% [50,51].

A MC study shows a peaking background from the process $K_S^0 K_L^0 \pi^0$ at a c.m. energy of 3.08 GeV. However, the contribution normalized according to the integrated data luminosity is expected to be only 2.6 events. To compensate for a possible incomplete simulation, such as an incorrect angular distribution, the systematic uncertainty from the possible $K_S^0 K_L^0 \pi^0$ background is increased to 3.1% assuming the background level might be higher by 50%.

All the systematic uncertainties are listed in Table II. The total systematic uncertainty is obtained by summing the individual contributions in quadrature.

B. Line shape

The line shape of the Born cross section of $e^+e^- \to K_S^0 K_L^0$, obtained from the results given in Table I, is

TABLE II. The relative systematic uncertainties (in %) from the K_S^0 selection [$\epsilon(K_S^0)$], E/cp, the ISR and VP correction factor $(1+\delta)$, the luminosity ($\mathcal{L}$) and the fit on the invariant mass of $\pi^+\pi^-$ pair (Fit). The column peak denotes the source from the peaking background and it has been estimated only at the c.m. energy of 3.08 GeV as elucidated in the text. The total systematic uncertainty is calculated by summing the individual contributions in quadrature. The relative statistical uncertainty is shown in the last column.

$\sqrt{s}$ (GeV)	$\epsilon(K_S^0)$	E/cp	$\epsilon(1+\delta)$	$\mathcal{L}$	Fit	Peak	Total systematic uncertainty	Relative statistical uncertainty
2.0000	2.99	0.75	0.63	0.89	6.87	⋯	7.6	9.7
2.0500	3.02	0.75	0.42	0.90	7.74	⋯	8.4	17.7
2.1000	2.92	0.75	0.52	0.89	15.14	⋯	15.5	12.9
2.1250	2.82	0.75	0.67	0.69	7.54	⋯	8.1	5.2
2.1500	2.82	0.75	0.82	0.89	8.93	⋯	9.4	42.9
2.1750	3.47	0.75	0.65	0.90	13.47	⋯	14.0	14.9
2.2000	3.47	0.75	0.52	0.89	5.42	⋯	6.5	13.6
2.2324	4.12	0.75	0.72	0.90	7.63	⋯	8.8	12.2
2.3094	3.17	0.75	0.94	0.89	5.24	⋯	6.2	11.2
2.3864	2.23	0.75	1.02	0.90	20.65	⋯	20.8	25.9
2.3960	3.51	0.75	0.95	0.89	13.25	⋯	13.8	14.3
2.6444	3.38	0.75	0.03	0.89	14.60	⋯	15.0	17.3
2.6464	3.38	0.75	0.03	0.89	3.81	⋯	5.2	15.8
2.9000	2.63	0.75	0.04	0.89	12.98	⋯	13.3	20.9
3.0800	4.8	0.75	0.04	0.84	14.75	3.1	15.6	19.1

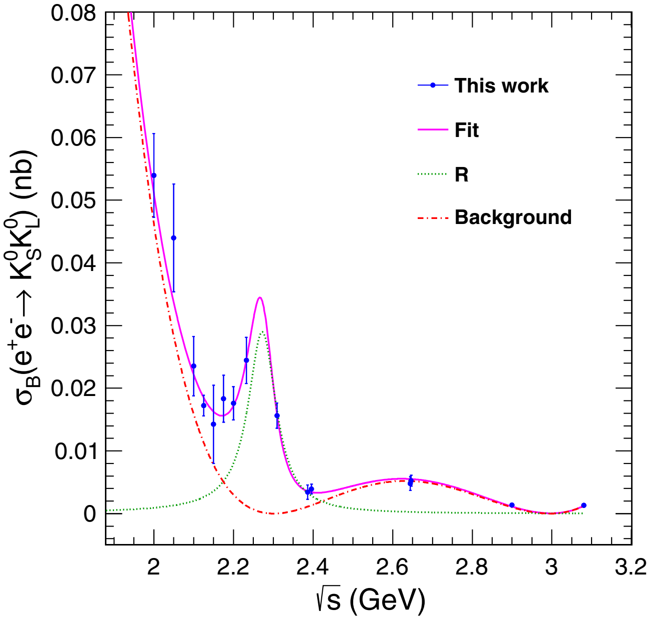

FIG. 4. Line shape of the process $e^+e^- \to K_S^0 K_L^0$ and fit curves. Points are data, solid curve shows the fit result, the dotted curve denotes the signal component and the dash-dotted line is the polynomial contribution.

displayed in Fig. 4. A resonance structure R around 2.2 GeV is observed. The cross section data are fitted by

$$\sigma_B = \frac{M^2 \beta(s)^3}{s\beta(M^2)^3} |\sqrt{\sigma} BW(s) + P(s)e^{i\phi}|^2, \qquad (2)$$

where $\beta(s) = \sqrt{1-4m^2_{K_S^0}/s}$; s is the square of the c.m. energy; $BW(s) = M\Gamma/(M^2 - s - i\sqrt{s}\Gamma)$ is a Breit-Wigner function describing the resonance; M, Γ and σ are the mass, width and peak cross section of the resonance, respectively; $P(s) = c_{p_0} + c_{p_1}\sqrt{s} + c_{p_2}s$ is a second-order polynomial function that is used to describe the nonresonant contribution, c_{p_i} corresponds to the coefficient of the ith-degree polynomial function, and ϕ is the relative phase between nonresonant and resonant amplitudes.

The least-squares (χ^2) method is used to perform the fit with both statistical and systematic uncertainties taken into account. The χ^2 is obtained via a matrix [see Eq. (1) in Ref. [63] and Eq. (2) in Ref. [64]] in which correlation effects of the various terms are included. Uncertainties from the K_S^0-selection efficiency, $1+\delta$, luminosity and ϵ are considered to be correlated, while the remaining ones are treated as uncorrelated. The line shape and the individual contributions obtained from the fit are shown in Fig. 4.

The mass and width of the structure determined by the fit are $M = 2273.7 \pm 5.7$ MeV$/c^2$ and $\Gamma = 86 \pm 44$ MeV, respectively, where the uncertainties are statistical. The goodness of the fit is $\chi^2/NDF = 4.6/8$, and the statistical significance of the structure is 7.5σ.

Various sources of systematic uncertainties of the observed structure are considered including those associated with the choice of the model used to describe the nonresonant component, the description of its width and the chosen fit range. To estimate the systematic uncertainties, we changed the description of the nonresonant component to a coherent sum of a second-order polynomial and continuum functions

$$P(s) = P'(s)e^{i\phi} + c_c(\sqrt{s})^{\alpha} e^{i\phi_c}, \qquad (3)$$

where $P'(s)$ and ϕ are the same as those defined in Eq. (2) but only used in the fit when $\sqrt{s} < c_{p_2}$, c_c is the coefficient of the continuum function and ϕ_c is the relative phase between continuum and resonant amplitudes. The term $P'(s)$ is used to account for unknown contributions. We note that for the previously published analysis of the $e^+e^- \to K^+K^-$ channel by BESIII [13], the same form was chosen, as presented by Eq. (3), to describe the nonresonant background contribution. The differences in the values of the peak cross section, mass, and width with respect to the nominal ones are $\Delta\sigma = 0.0150$ nb, $\Delta m = 17.7$ MeV$/c^2$, and $\Delta\Gamma = 8.4$ MeV, respectively. By replacing the description of the width with an energy dependent one $[\Gamma(s,m) = \Gamma \times \frac{s}{m_R^2}(\frac{\beta(s,m_K^0)}{\beta(m^2,m_K^0)})^3]$ in Eq. (2), the peak cross section, mass, and width change by an amount of $\Delta\sigma = 0.0001$ nb, $\Delta m = 2.2$ MeV$/c^2$, and $\Delta\Gamma = 0.3$ MeV, respectively. Uncertainties from the fit range are estimated by excluding the point at the c.m. energy of 2.00 GeV or the one at 3.08 GeV. $\Delta\sigma_1$ and $\Delta\sigma_2$ (Δm_1 and Δm_2, $\Delta\Gamma_1$ and $\Delta\Gamma_2$) denote the differences of the peak cross sections (masses and widths) obtained by fitting all energy points with a fit excluding those two energy points. Systematic uncertainties associated with the fit range on the mass and width are subsequently estimated by $\sqrt{(\Delta\sigma_1)^2 + (\Delta\sigma_2)^2} = 0.0030$ nb, $\sqrt{(\Delta m_1)^2 + (\Delta m_2)^2} = 7.5$ MeV$/c^2$, and $\sqrt{(\Delta\Gamma_1)^2 + (\Delta\Gamma_2)^2} = 50.2$ MeV. Total systematic uncertainties are obtained by taking the quadratic sum of all the differences, which amount to 0.0153 nb, 19.3 MeV$/c^2$, and 50.9 MeV on the peak cross section, mass, and width, respectively. Only the statistic uncertainty on ϕ is considered.

$\Gamma_{e^+e^-}Br_{K_S^0K_L^0}$ of the resonance R is calculated from the peak cross section by making use of $\sigma_R = 12\pi C\Gamma_{e^+e^-}Br_{K_S^0K_L^0}/(\Gamma M^2)$ [47], where σ_R represents the peak cross section obtained through Eq. (2), $Br_{K_S^0K_L^0}$ is the branching fraction of $R \to K_S^0K_L^0$, $\Gamma_{e^+e^-}$ is partial width of $R \to e^+e^-$, M and Γ are the mass and width of the resonance, and $C = 0.3894 \times 10^{12}$ nb MeV$^2/c^4$ [60]. $\Gamma_{e^+e^-}Br_{K_S^0K_L^0}$ for the process is obtained from the fit results and listed in Eq. (4).

The χ^2 obtained by the earlier-described matrix may cause a bias in the fit [63–66]. To estimate the bias effect, an unbiased χ^2 definition [Eq. (7) in Ref. [66]] is used to fit the line shape. The differences between the two cases are negligible in this analysis.

The parameters of the resonance around 2.2 GeV are

$$\begin{aligned} M &= 2273.7 \pm 5.7 \pm 19.3\ \mathrm{MeV}/c^2, \\ \Gamma &= 86 \pm 44 \pm 51\ \mathrm{MeV}, \\ \sigma &= 0.0289 \pm 0.0125 \pm 0.0153\ \mathrm{nb}, \\ \Gamma_{e^+e^-} \text{-} Br_{K_S^0 K_L^0} &= 0.9 \pm 0.6 \pm 0.7\ \mathrm{eV}, \\ \phi &= 81.1 \pm 17.4\ \ \mathrm{deg}, \\ \text{or} &\quad -98.9 \pm 23.0\ \ \mathrm{deg}, \end{aligned} \tag{4}$$

where the quoted uncertainties are statistical and systematic, respectively. The mass and width are consistent within 2σ with measurements of the mass and width of a similar structure observed in $e^+e^- \to K^+K^-$ at BESIII [13], which gave $M = 2239.2 \pm 7.1 \pm 11.3\ \mathrm{MeV}/c^2$ and $\Gamma = 139.8 \pm 12.3 \pm 20.6$ MeV.

VI. SUMMARY

We report a measurement of the Born cross sections in $e^+e^- \to K_S^0 K_L^0$ from $\sqrt{s} = 2.00$ to 3.08 GeV obtained at fifteen energy points with BESIII. The data are consistent within 2σ with previous measurements by the *BABAR* Collaboration [37] in the overlap region from 2.00 to 2.54 GeV, but with a significantly improved precision as demonstrated in Figure 4. Moreover, the Born cross sections from 2.54 to 3.08 GeV are reported for the first time. A structure is observed around 2.2 GeV, which is similar to the one observed earlier in $e^+e^- \to K^+K^-$ [13]. The results of both processes taken with BESIII and *BABAR* are shown in Fig. 5 for comparison.

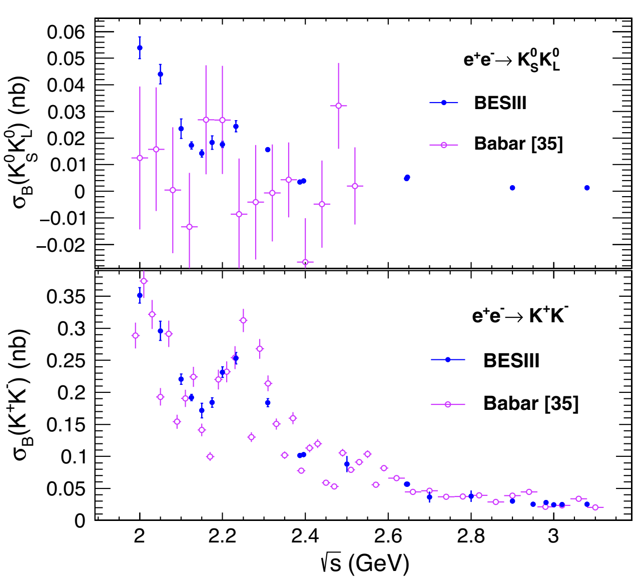

FIG. 5. Comparison of cross section measurements of the processes $e^+e^- \to K_S^0 K_L^0$ (top panel) and $e^+e^- \to K^+K^-$ (bottom panel) by BESIII (filled dots) [13] and *BABAR* (open circles) [37].

A fit is applied to the data, where the mass and width of the resonance are determined to be $M = 2273.7 \pm 5.7 \pm 19.3\ \mathrm{MeV}/c^2$ and $\Gamma = 86 \pm 44 \pm 51$ MeV, respectively. In addition, $\Gamma_{e^+e^-}\text{-}Br_{K_S^0 K_L^0}$ is found to be $0.9 \pm 0.6 \pm 0.7$ eV. The first uncertainties in the parameters are statistical and the second ones are systematic. The mass and width are consistent within 2σ and 1σ, respectively, with the resonance parameters obtained by fitting the cross sections for the process $e^+e^- \to K^+K^-$ ($M = 2239.2 \pm 7.1 \pm 11.3\ \mathrm{MeV}/c^2$ and $\Gamma = 139.8 \pm 12.3 \pm 20.6$ MeV) [13].

The mass of our observed resonance is compatible within 2σ with the PDG-evaluated mass of the $\phi(2170)1^{--}$ candidate ($2160 \pm 80\ \mathrm{MeV}/c^2$) [60]. Our width is consistent within 1σ to the PDG-evaluated width of the $\phi(2170)$ [60]. The compatibility of our resonance parameters with the $\rho(2150)1^{--}$ candidate is less conclusive since its world average mass and width are not provided by the PDG [60]. We note, however, that our reported mass and width are consistent with the resonance-parameter measurements of the process $e^+e^- \to \gamma\pi^+\pi^-$ by *BABAR* [67]. Our conclusions with respect to the $\phi(2170)$ and $\rho(2150)$ properties are compatible with those reported in the $e^+e^- \to K^+K^-$ study by BESIIII [13]. The limited statistics, especially for the cross section measurements above 2.4 GeV, make it difficult to discuss in more detail the observed structure reported in this paper.

ACKNOWLEDGMENTS

We appreciate Prof. Dianyong Chen from Southeast University (SEU) for the important discussions and suggestions. The BESIII Collaboration thanks the staff of BEPCII and the IHEP computing center and the supercomputing center of USTC for their strong support. This work is supported in part by National Key R&D Program of China under Contracts No. 2020YFA0406400, No. 2020YFA0406300, No. 2015CB856700; National Natural Science Foundation of China (NSFC) under Contracts No. 11625523, No. 11635010, No. 11735014, No. 11822506, No. 11835012, No. 11935015, No. 11935016, No. 11935018, No. 11961141012; the Chinese Academy of Sciences (CAS) Large-Scale Scientific Facility Program; Joint Large-Scale Scientific Facility Funds of the NSFC and CAS under Contracts No. U1732263, No. U1832207 and No. U2032115; CAS Key Research Program of Frontier Sciences under Contracts No. QYZDJ-SSW-SLH003, No. QYZDJ-SSW-SLH040; 100 Talents Program of CAS; The Institute of Nuclear and Particle Physics (INPAC) and Shanghai Key Laboratory for Particle Physics and Cosmology; ERC under Contract No. 758462; German Research Foundation DFG under Contract No. 443159800. Collaborative Research Center CRC 1044, FOR 2359; Istituto

Nazionale di Fisica Nucleare, Italy; Ministry of Development of Turkey under Contract No. DPT2006K-120470; National Science and Technology fund; STFC (United Kingdom); The Knut and Alice Wallenberg Foundation (Sweden) under Contract No. 2016.0157; The Royal Society, UK under Contracts No. DH140054, No. DH160214; The Swedish Research Council; U.S. Department of Energy under Contracts No. DE-FG02-05ER41374, No. DE-SC-0012069. This paper is also supported by the NSFC under Contracts No. 11605074, No. 11335008, No. 12105276.

[1] B. Aubert *et al.* (*BABAR* Collaboration), Phys. Rev. D **74**, 091103 (2006).
[2] M. Ablikim *et al.* (BES Collaboration), Phys. Rev. Lett. **100**, 102003 (2008).
[3] C. P. Shen *et al.* (Belle Collaboration), Phys. Rev. D **80**, 031101 (2009).
[4] J. P. Lees *et al.* (*BABAR* Collaboration), Phys. Rev. D **86**, 012008 (2012).
[5] B. Aubert *et al.* (*BABAR* Collaboration), Phys. Rev. D **77**, 092002 (2008).
[6] B. Aubert *et al.* *BABAR* Collaboration), Phys. Rev. D **76**, 012008 (2007).
[7] M. Ablikim *et al.* (BESIII Collaboration), Phys. Rev. D **91**, 052017 (2015).
[8] M. Ablikim *et al.* (BESIII Collaboration), Phys. Rev. D **100**, 032009 (2019).
[9] M. Ablikim *et al.* (BESIII Collaboration), Phys. Rev. Lett. **124**, 112001 (2020).
[10] M. Ablikim *et al.* (BESIII Collaboration), Phys. Rev. D **102**, 012008 (2020).
[11] M. Ablikim *et al.* (BESIII Collaboration), Phys. Rev. D **99**, 012014 (2019).
[12] M. Ablikim *et al.* (BESIII Collaboration), Phys. Lett. B **813**, 136059 (2021).
[13] M. Ablikim *et al.* (BESIII Collaboration), Phys. Rev. D **99**, 032001 (2019).
[14] M. Ablikim *et al.* (BESIII Collaboration), Phys. Rev. D **103**, 072007 (2021).
[15] M. Ablikim *et al.* (BESIII Collaboration), Phys. Rev. D **104**, 032007 (2021).
[16] Z. G. Wang, Nucl. Phys. **A791**, 106 (2007).
[17] S. S. Agaev, K. Azizi, and H. Sundu, Phys. Rev. D **101**, 074012 (2020).
[18] H. W. Ke and X. Q. Li, Phys. Rev. D **99**, 036014 (2019).
[19] R. R. Dong, N. Su, H. X. Chen, E. L. Cui, and Z. Y. Zhou, Eur. Phys. J. C **80**, 749 (2020).
[20] F. X. Liu, M. S. Liu, X. H. Zhong, and Q. Zhao, Phys. Rev. D **103**, 016016 (2021).
[21] C. Deng, J. Ping, F. Wang, and T. Goldman, Phys. Rev. D **82**, 074001 (2010).
[22] N. V. Drenska, R. Faccini, and A. D. Polosa, Phys. Lett. B **669**, 160 (2008).
[23] G. J. Ding and M. L. Yan, Phys. Lett. B **650**, 390 (2007).
[24] G. J. Ding and M. L. Yan, Phys. Lett. B **657**, 49 (2007).
[25] J. J. Dudek, Phys. Rev. D **84**, 074023 (2011).
[26] J. Ho, R. Berg, T. G. Steele, W. Chen, and D. Harnett, Phys. Rev. D **100**, 034012 (2019).
[27] E. Klempt and A. Zaitsev, Phys. Rep. **454**, 1 (2007).
[28] L. Zhao, N. Li, S. L. Zhu, and B. S. Zou, Phys. Rev. D **87**, 054034 (2013).
[29] Y. Yang, D. Y. Chen, and Z. Lu, Phys. Rev. D **100**, 073007 (2019).
[30] A. Martinez Torres, K. P. Khemchandani, L. S. Geng, M. Napsuciale, and E. Oset, Phys. Rev. D **78**, 074031 (2008).
[31] L. Alvarez-Ruso, J. A. Oller, and J. M. Alarcon, Phys. Rev. D **80**, 054011 (2009).
[32] T. Barnes, N. Black, and P. R. Page, Phys. Rev. D **68**, 054014 (2003).
[33] C. Q. Pang, Phys. Rev. D **99**, 074015 (2019).
[34] Q. Li, L. C. Gui, M. S. Liu, Q. F. Lü, and X. H. Zhong, Chin. Phys. C **45**, 023116 (2021).
[35] X. Wang, Z. F. Sun, D. Y. Chen, X. Liu, and T. Matsuki, Phys. Rev. D **85**, 074024 (2012).
[36] J. Z. Wang, L. M. Wang, X. Liu, and T. Matsuki, Phys. Rev. D **104**, 054045 (2021).
[37] J. P. Lees *et al.* (*BABAR* Collaboration), Phys. Rev. D **101**, 012011 (2020).
[38] D. Y. Chen, J. Liu, and J. He, Phys. Rev. D **101**, 074045 (2020).
[39] C. Q. Pang, Y. R. Wang, J. F. Hu, T. J. Zhang, and X. Liu, Phys. Rev. D **101**, 074022 (2020).
[40] F. Mane, D. Bisello, J. C. Bizot, J. Buon, A. Cordier, and B. Delcourt, Phys. Lett. **99B**, 261 (1981).
[41] P. M. Ivanov, L. M. Kurdadze, M. Y. Lelchuk, E. V. Pakhtusova, V. A. Sidorov, A. N. Skrinsky, A. G. Chilingarov, Y. M. Shatunov, B. A. Shvarts, and S. I. Eidelman, JETP Lett. **36**, 112 (1982), https://www.hepdata.net/record/ins185077.
[42] R. R. Akhmetshin *et al.* (CMD-2 Collaboration), Phys. Lett. B **466**, 385 (1999); **508**, 217(E) (2001).
[43] R. R. Akhmetshin, V. M. Aulchenko, V. S. Banzarov, L. M. Barkov, S. E. Baru, N. S. Bashtovoy, A. E. Bondar, D. V. Bondarev, A. V. Bragin, S. K. Dhawan *et al.*, Phys. Lett. B **551**, 27 (2003).
[44] R. R. Akhmetshin *et al.* (CMD-2 Collaboration), Phys. Lett. B **578**, 285 (2004).
[45] M. N. Achasov, K. I. Beloborodov, A. V. Berdyugin, A. G. Bogdanchikov, A. V. Bozhenok, A. D. Bukin, D. A. Bukin, S. V. Burdin, T. V. Dimova and V. P. Druzhinin *et al.*, Phys. Rev. D **63**, 072002 (2001).
[46] M. N. Achasov, K. I. Beloborodov, A. V. Berdyugin, A. V. Bozhenok, D. A. Bukin, T. V. Dimova, V. P. Druzhinin, V. B. Golubev, I. A. Koop, A. A. Korol *et al.*, J. Exp. Theor. Phys. **103**, 720 (2006).

[47] J. P. Lees *et al.* (*BABAR* Collaboration), Phys. Rev. D **89**, 092002 (2014).
[48] M. Ablikim *et al.* (BESIII Collaboration), Nucl. Instrum. Methods Phys. Res., Sect. A **614**, 345 (2010).
[49] C. Yu, Z. Duan, S. Gu, Y. Guo, X. Huang, D. Ji, H. Ji, Y. Jiao, Z. Liu, Y. Peng *et al.*, Proceedings of IPAC2016, Busan, Korea, 2016, https://accelconf.web.cern.ch/ipac2016/doi/JACoW-IPAC2016-TUYA01.html.
[50] M. Ablikim *et al.* (BESIII Collaboration), Chin. Phys. C **41**, 063001 (2017).
[51] M. Ablikim *et al.* (BESIII Collaboration), Chin. Phys. C **41**, 113001 (2017).
[52] S. Agostinelli *et al.* (GEANT4 Collaboration) Nucl. Instrum. Methods Phys. Res., Sect. A **506**, 250 (2003).
[53] Z. Y. Deng *et al.*, Chin. Phys. C **30**, 371 (2006), http://hepnp.ihep.ac.cn/en/article/id/283d17c0-e8fa-4ad7-bfe3-92095466def1.
[54] R. G. Ping, Chin. Phys. C **38**, 083001 (2014).
[55] G. Balossini, C. M. Carloni Calame, G. Montagna, O. Nicrosini, and F. Piccinini, Nucl. Phys. **B758**, 227 (2006).
[56] B. Andersson and H. M. Hu, arXiv:hep-ph/9910285.
[57] S. Nova, A. Olchevski, and T. Todorov, Report No. DELPHI-90-35 PROG 152.
[58] M. Xu, K. L. He, Z. P. Zhang, Y. F. Wang, J. M. Bian, G. F. Cao, X. X. Cao, S. J. Chen, Z. Y. Deng, C. D. Fu *et al.*, Chin. Phys. C **33**, 428 (2009).
[59] M. Xu, K. L. He, Z. P. Zhang, Y. F. Wang, J. M. Bian, C. D. Fu, B. Huang, X. B. Ji, S. S. Sun, L. Yan *et al.*, Chin. Phys. C **34**, 92 (2010).
[60] P. A. Zyla *et al.* (Particle Data Group), Prog. Theor. Exp. Phys. **2020**, 083C01 (2020).
[61] X. Zhou, S. Du, G. Li, and C. Shen, Comput. Phys. Commun. **258**, 107540 (2021).
[62] M. Ablikim *et al.* (BESIII Collaboration), Phys. Rev. Lett. **109**, 042003 (2012).
[63] X. H. Mo and Y. S. Zhu, Chin. Phys. C **27**, 371 (2003), http://hepnp.ihep.ac.cn/en/article/id/3b0d9cec-e6d8-4f3e-ae03-43a716d83ed4.
[64] X. H. Mo, Chin. Phys. C **30**, 140 (2006), http://hepnp.ihep.ac.cn/en/article/id/6965e096-33eb-49f5-8315-8cfc7937bf51.
[65] X. H. Mo and Y. S. Zhu, Chin. Phys. C **27**, 747 (2003), http://hepnp.ihep.ac.cn/en/article/id/41f9656d-2ec6-4ae1-8514-610e23f85c0d.
[66] X. H. Mo, Chin. Phys. C **31**, 745 (2007), http://hepnp.ihep.ac.cn/en/article/id/3a9524db-6254-4680-9e87-4693cd2cd82a.
[67] J. P. Lees *et al.* (*BABAR* Collaboration), Phys. Rev. D **86**, 032013 (2012).